Available online at www.sciencedirect.com
SCIENCE DIRECT
Biochimica et Biophysica Acta 1763 (2006) 110 – 119
BIOCHIMICA ET BIOPHYSICA ACTA
BBA
http://www.elsevier.com/locate/bba

# The induction of NOS2 expression by the hybrid cecropin A–melittin antibiotic peptide CA(1–8)M(1–18) in the monocytic line RAW 264.7 is triggered by a temporary and reversible plasma membrane permeation

Cristina Arias [a], Miriam Guizy [a], Juan R. Luque-Ortega [b], Esther Guerrero [b], Beatriz G. de la Torre [c], David Andreu [c], Luis Rivas [b,*], Carmen Valenzuela [a,*]

[a] *Institute of Pharmacology and Toxicology, CSIC/UCM, School of Medicine, Universidad Complutense, 28040 Madrid, Spain*
[b] *Centro de Investigaciones Biológicas (CSIC), Ramiro de Maeztu 9, 28040 Madrid, Spain*
[c] *Department of Experimental and Health Sciences, Pompeu Fabra University, 08003 Barcelona, Spain*

Received 8 August 2005; received in revised form 25 October 2005; accepted 7 November 2005
Available online 9 December 2005

**Abstract**

There is an increasing awareness of immune cell modulation by antimicrobial peptides. While this process often requires specific receptors for the peptides involved, several reports point out to a receptor-independent process. The cecropin A–melittin hybrid peptide CA(1–8)M(1–18) (KWKLFKKIGIGAVLKVLTTGLPALIS-amide) modifies gene expression in the macrophage line RAW 264.7 in the absence of any previous macrophage priming, suggesting a membrane permeation process. To further analyze the initial steps of this mechanism, we have studied the interaction of the peptide with these cells. Below 2 μM, CA(1–8)M(1–18) causes a concentration-dependent membrane depolarization partially reversible with time. At 2 μM, the accumulation of the SYTOX green vital dye is one half of that achieved with 0.05% Triton X-100. The binding level, as assessed by fluorescein-labeled CA(1–8)M(1–18), varies from $7.7 \pm 1.2$ to $37.4 \pm 3.9 \times 10^6$ molecules/cell over a 0.5–4.0 μM concentration range. Electrophysiological experiments with 0.5 μM CA(1–8)M(1–18), a concentration that triggers maximal NOS2 expression and minimal toxicity, show a reversible current induction in the RAW 264.7 plasma membrane that is maintained as far as peptide is present. This activation of the macrophage involves the production of nitric oxide, a metabolite lethal for many pathogens that results from unspecific membrane permeation by antimicrobial peptides, and represents a new mode of action that may open new therapeutic possibilities for these compounds against intracellular pathogens.


*Keywords:* Antimicrobial peptide; Macrophage; Cecropin A–melittin; Electrophysiology

## 1. Introduction

Eukaryotic antibiotic peptides (EAPs) are key components of innate immunity. They are ubiquitous in all pluricellular organisms, where they act as a first defensive barrier against invading pathogens [1,2]. Despite their broad structural variety, most of them share a tendency to adopt amphipathic structures upon contact with the pathogen and a marked cationic character [3,4]. For most EAPs, the lethal mechanism consists in the permeabilization of the pathogen plasma membrane, by stoichiometric interaction with the acidic phospholipids exposed at the outer leaflet of the membrane. This phospholipid distribution is specific of prokaryotes and lower eukaryotes, in contrast with higher eukaryotes where the anionic phospholi-

*Abbreviations:* Bisoxonol, bis-(1,3-diethylthiobarbituric) trimethine oxonol; CA(1-8)M(1-18), KWKLFKKIGIGAVLKVLTTGLPALIS-amide; CCR6, chemokine receptor 6; CFSE [5-(and-6), carboxyfluorescein diacetate succinimidyl ester; EAPs, eukaryotic antimicrobial peptides; HIFCS, heat inactivated fetal calf serum (HIFCS); HBD, human β-defensin; LPS, human lipopolysaccharide; MALDI-TOF, matrix-assisted laser desorption ionization, time-of-flight (mass spectrometry); mβD, mouse β-defensin; NF-κB, nuclear factor kappa B

* Corresponding authors. L. Rivas is to be contacted at Centro de Investigaciones Biológicas (CSIC), Ramiro de Maeztu 9, 28040 Madrid, Spain. Tel.: +34 91 837 3112; fax: +34 91 536 0432. C. Valenzuela, Institute of Pharmacology and Toxicology, CSIC/UCM, School of Medicine. Universidad Complutense, 28040 Madrid, Spain. Tel.: +34 91 394 7168; fax: +34 91 394 1470.

*E-mail addresses:* luis.rivas@cib.csic.es (L. Rivas), carmenva@med.ucm.es (C. Valenzuela).

0167-4889/$ - see front matter © 2005 Elsevier B.V. All rights reserved.
doi:10.1016/j.bbamcr.2005.11.003

pids are confined to the cytoplasmic face of the membrane, precluding interaction with EAPs [4–6].

Aside from this main function of EAPs as early host defense components, there is growing evidence for their involvement in other physiological processes such as chemotaxis, scarification, angiogenesis or productive interaction with effector cells of the immune system [7–9]. Some of these newly found roles have been experimentally elucidated for specific EAPs or closely related analogues, and involve receptors and signaling pathways [10] for the target cells under study, even with a different zoological origin as the EAP assayed [9]. For instance, for the EAP LL-37 it was conclusively proven that both chemotactic and angiogenic activities were performed through the G-protein coupled formyl peptide receptor-like 1 [11], or that the binding of some human or mouse β-defensins to the CCR6 chemokine receptor drove a chemotactic response [7]. This is in sharp contrast with microbicidal effects, which largely involve loose patterns of pathogen recognition. On the other hand, although the dogma of preferential permeabilization of pathogen or transformed-cell plasma membrane as the rationale for EAP cellular specificity remains basically valid, it is challenged by the non-lethal permeabilization of higher eukaryotic cells by a wide variety of EAPs, including magainins on non-transformed fibroblasts [12], or β-defensin 3 [13] or protegrins [14] on *Xenopus* oocytes. These last results, however, were often obtained in the course of studies on cell permeation by EAPs, hence at peptide/cell ratios much higher than required for microbicidal activity. In other cases, however, a real biological function seems to exist for these permeations, since they were observed at a physiological range of concentrations for the selected peptide. Examples of this trend are the permeation of intestinal epithelial cells by cryptdins, causing chloride [15], and IL-8 [16] secretion, the vascular permeability induced by the CAP heparin-binding protein from neutrophils upon its activation through adhesion to the vascular epithelia [17], or the unspecific permeabilization of human LPS-primed monocytes by LL-37, leading to the release of intracellular ATP, which in turn binds into the P2X7 purinergic receptor [18], acting as autocrine or paracrine signal to these cells to induce IL-1β processing and release.

The cecropin A (CA)–melittin (M) hybrid peptides, in which the juxtaposition of N-terminal sequences of the insect antibiotic cecropin A with those of the bee venom toxin melittin produces substantially improved activities over the parent structures [19], show high bactericidal, antiendotoxic, fungicidal and leishmanicidal activities, both in vitro [20,21] and in vivo [22–24]. We have also found that CA(1–8)M(1–18), an analogue where the first eight residues of cecropin A are followed by the first eighteen from melittin, induces expression of NOS2 in the murine macrophage line RAW 264.7 in the absence of any previous priming by LPS or cytokines [25]. This effect is accompanied by a rise in intracellular $Ca^{2+}$ concentration immediately after peptide addition and prevented by the presence of EGTA in the incubation media, ruling out $Ca^{2+}$ release from intracellular stores. Since the all-D enantiomer of CA(1–8)M(1–18) retains this activity, the involvement of a specific receptor was excluded and plasma membrane permeation validated as the most likely cause. The hypothesis was further supported by the fact that the peptide permeated zwitterionic liposomes mimicking the plasma membrane composition of higher eukaryotes [26].

In order to gain further insight into the early steps of the CA(1–8)M(1–18)-RAW 264.7 interaction, we have used a combination of patch-clamp, membrane permeation and confocal microscopy techniques. Our results support a process of transient depolarization of the macrophage plasma membrane, without significant cytotoxicity, as the driving force for this indirect mechanism of defense, and suggest new, unexpected roles for CA(1–8)M(1–18) modulation of the immune response.

## 2. Materials and methods

### 2.1. Reagents

Chemicals of the best available quality were purchased from Sigma (St. Louis, MO) and Fluka (Buchs, Switzerland). Bisoxonol, [bis-(1,3-diethylthiobarbituric) trimethine oxonol], SYTOX® green, and CFSE [5-(and-6) carboxyfluorescein diacetate succinimidyl ester] were from Molecular Probes (Leiden, The Netherlands). Peptides were synthesized by the solid phase method [27] using Fmoc chemistry [28], purified by reverse-phase HPLC (purity >95%) and characterized by amino acid analysis and MALDI-TOF mass spectrometry. A fluorescent analogue of CA(1–8)M(1–18) was made by N-terminal extension with 6-aminohexanoic acid to which fluorescein was coupled.

### 2.2. Plasmids

The vectors piNOS2luc and pNF3ConA-luc have been described [29,30]. Both encode the *Photinus pyralis* luciferase gene as reporter, under the control of either the 5 proximal flanking region of the murine promoter for NOS2 (piNOSLuc [29]), or of a promoter containing three copies of the κB consensus from the immunoglobulin kappa-chain promoter (pNF3ConA-luc) [30]. Both plasmids were kindly provided by Prof. Manuel Fresno (Center for Molecular Biology CSIC, Madrid Spain).

### 2.3. Cell culture

RAW 264.7 cells were cultured in RPMI 1640 (Gibco, BRL, Gaithesburg, MD) supplemented with 10% heat inactivated fetal calf serum (HIFCS) (Gibco, BRL), L-glutamine (2 mM), gentamicin (30 μg/mL) and penicillin (100 IU/mL) (Sigma). Cultures were passed every 3 to 5 days and cells were detached by a brief trypsin treatment, visualized in an inverted microscope. Cells for patch-clamp experiments were removed from the dish with a rubber policeman, a procedure that left the vast majority of cells intact. The cell suspension was stored at room temperature (21–23 °C) and used within 6 h.

### 2.4. Cell transfection

The RAW 264.7 cells were transfected according to supplier's (GIBCO, BRL, Paisley, UK) instructions. Briefly, two 50 μL aliquots of lipofectin (3% v/v) and the respective plasmid (0.15 μg) in RPMI 1640 were separately preincubated at 24 °C, gently mixed and incubated for 15 min at 24 °C. The mixture was added to the cells (400 μL, $1.5 \times 10^6$ cells/mL in RPMI 1640 without serum, 6 h, 37 °C, 5% $CO_2$). Upon transfection, cells were washed, resuspended in RPMI 1640+10% HIFCS and transferred into a 24-well microplate. After overnight incubation, the medium was replaced with an identical amount containing the respective concentration of CA(1–8)M(1–18) or, as a positive control, LPS from *Salmonella typhimurium* (Sigma) at a final concentration of 1 μg/mL. Finally, the cells were incubated for an additional 24 h. Luciferase activity was evaluated by the Luciferase Assay System (Promega Biotech, Barcelona, Spain) after lysis of the cells using the regents included in the kit. Measurements were taken every 30 s in a TD-20/20 luminometer (Turner Design, Sunnyvale, CA). Values were expressed as the fold increase relative to cells in the absence of stimuli.

### 2.5. Plasma membrane permeabilization of RAW 264.7 cells by CA(1–8)M(1–18)

Two sets of complementary experiments were carried out: plasma membrane permeation to the vital dye SYTOX® green, and depolarization. In both cases, RAW 264.7 cells were harvested, washed, and resuspended in RPMI-1640+2% HIFCS, transferred into 96-well microplates ($5 \times 10^4$ cells/well), and allowed to adhere overnight. Afterwards, cells were washed three times with 300 μL of Hanks+Glc through pipette aspiration. To assess membrane permeation to the vital dye, 100 μL of 2 μM SYTOX® green in Hanks+Glc were added to the well, and the dye fluorescence monitored in a Polarstar Galaxy microplate reader (BMG Labotechnologies, Offenburg, Germany), equipped with 485 and 520 nm filters as excitation and emission wavelengths, respectively. Once the fluorescence value reached stabilization, 100 μL of peptide solution in Hanks+Glc were added (final peptide concentrations 0.1–15 μM), and changes in fluorescence monitored. Complete permeation was defined as that obtained after addition of Triton X-100 at 0.05%. Experiments were carried out in triplicate at 37 °C.

A similar protocol was followed to assess RAW 264.7 plasma membrane depolarization [31]. Once the cells were washed as above, 100 μL of 0.2 μM bisoxonol in Hanks+Glc were added. Cells were incubated for an additional 25 min to allow dye equilibration, and 100 μL of the peptide solution were then added. Increase in fluorescence ($\lambda_{exc}$=544 and $\lambda_{em}$=584 nm) due to dye insertion into the hydrophobic matrix of the membrane once depolarized, was monitored in a Polarstar Galaxy fluorescence microplate reader at 37 °C.

### 2.6. Binding of fluoresceinated CA(1–8)M(1–18) to RAW 264.7 cells

Cells were plated at $5 \times 10^4$ cells/well in a 96-well microplate and allowed to adhere for 12 h, then incubated in Hanks+Glc for 4 h in the presence of 0.5 μM fluoresceinated CA(1–8)M(1–18) at 37 °C. Non-bound peptide was washed with 1 mL of Hanks medium, cells were solubilized by addition of SDS (final concentration 0.1%) and fluorescence measured in a Polarstar Galaxy microplate reader ($\lambda_{exc}$=494 nm, $\lambda_{em}$=599 nm). The number of bound molecules was calculated according to a standard curve of the fluoresceinated CA(1–8)M(1–18). For confocal microscopy, the protocols were identical except that the cells were seeded in a 8 multiwell chamber slide system (Nunc GmbH, Wiesbaden, Germany). After incubation with the peptide and further washing, cells were observed in a Leica TCS-SP2-AOBS-UV confocal microscope equipped with inverted optics (Leica DMIRE2) with excitation at 482 nm and emission at 519 nm. Three-dimensional reconstruction was carried out using the Leica confocal software v. 2.5.

### 2.7. CFSE labeling of RAW 264.7 cells

Cells were plated as above and incubated with 9 μM CFSE for 30 min at 37 °C [32]. The non-incorporated dye was removed by flushing the well with Hanks+Glc, and observed at the confocal microscope with the same settings than for fluoresceinated CA(1–8)M(1–18).

### 2.8. Electrophysiological technique and data acquisition

The intracellular pipette filling solution contained: 80 mM aspartate, 50 mM KCl, 3 mM phosphocreatine, 10 mM $KH_2PO_4$, 3 mM MgATP, 10 mM HEPES, 5 mM EGTA, and was adjusted to pH 7.25 with KOH. The bath solution contained: 130 mM NaCl, 4 mM KCl, 1.8 mM $CaCl_2$, 1 mM $MgCl_2$, 10 mM HEPES, and 10 mM D-glucose. The pH was adjusted to a final value of 7.40 with NaOH. Recordings were made with an Axopatch 200A patch-clamp amplifier (Axon Instruments, Foster City, CA) using the whole-cell configuration of the technique [33]. Currents were recorded at room temperature (21–23 °C) at a stimulation frequency of 0.1 Hz, and sampled at 2 kHz after anti-alias filtering at 1 kHz. Data acquisition and command potentials were controlled with the use of pCLAMP 6.0.1. (Axon Instruments). The average pipette resistance was 2.1±0.5 MΩ ($n$=14). Gigaohm seal formation was achieved by suction (10±1 GΩ, $n$=15). Capacitive surface area and access resistance were 4.6±0.6 pF ($n$=14) and 6.6±0.5 MΩ ($n$=14), respectively. Usually, 80% compensation of the effective access resistance was obtained, which led to a mean uncompensated access resistance of 5.6±0.6 MΩ ($n$=14). Since maximum current amplitudes averaged 0.8±0.2 nA ($n$=1 4), no significant voltage errors (<5 mV) were expected with this experimental setting. Microcal Origin 7.05 (Microcal Software, Northampton, MA), the CLAMPFIT utility of the pCLAMP 6.0.1. program and custom made programs were used to perform least-squares fitting and for data presentation.

### 2.9. Statistical analysis

Data are presented as mean values±S.D. Mean values in control conditions and in the presence of peptide for a single variable were compared by paired Student's $t$ test. One-way ANOVA was used to compare more than two groups. Statistical significance was set at $P<0.05$.

## 3. Results

### 3.1. Plasma membrane permeabilization of RAW 264.7 cells by CA(1–8)M(1–18)

In order to analyze the membrane-permeating effects of CA(1–8)M(1–18), two different but related parameters were measured.

First, we analyzed the depolarization carried out by the peptide, monitored by the increase in fluorescence of the potential-sensitive dye bisoxonol, as this parameter is directly related to the maintenance of ionic gradients across the plasma membrane, hence highly susceptible to changes in permeability to monovalent ions. CA(1–8)M(1–18) caused a fast and concentration-dependent depolarization on RAW 264.7 cells (Fig. 1). At CA(1–8)M(1–18) concentrations between 0.1 and 0.5 μM, an initial rise in the fluorescence of the potential-sensitive dye bisoxonol was observed, followed by a partial reversion towards the initial values, with an extent and a recovery time inversely proportional to peptide concentration. A full and irreversible depolarization, suggestive of permanent membrane damage, was only observed at peptide concentrations higher than 15 μM.

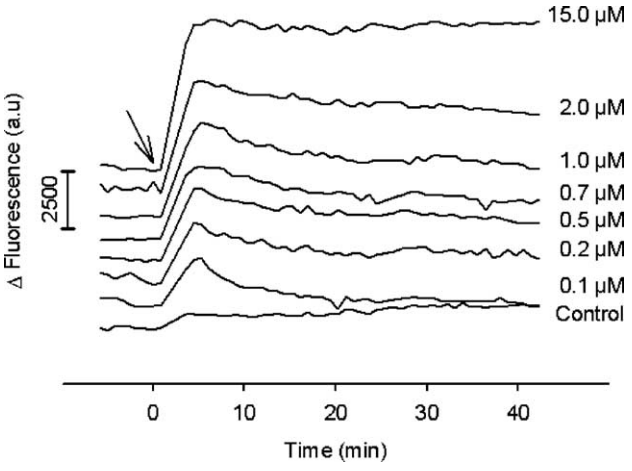


Fig. 1. Depolarization of RAW 264.7 cells by CA(1–8)M(1–18). Peptide was added to cells ($10^5$ cells/well) at the concentrations shown at the right of the respective trace, in the presence of 0.1 μM bisoxonol, and increase in fluorescence ($\lambda_{exc}$=544 nm, $\lambda_{em}$=584 nm) was monitored. Arrows indicate addition of peptide ($t$=0). Figure is representative of three other experiments performed independently.

Second, and in order to compare these effects with peptide cytotoxicity, the influx of the cationic vital dye SYTOX® green (MW=900) into the cytoplasm was monitored. This dye permeates cells with damaged plasma membrane, not intact organisms, and binds to intracellular nucleic acids with an enhancement of its fluorescence [34]. For CA(1–8)M(1–18) at concentrations above 0.2 μM (Fig. 2), such an increase in fluorescence was observed in a dose-dependent manner, though it never reached the full permeation levels achieved with 0.05% Triton X-100. For any given peptide concentration, once the respective maximal fluorescence value was reached, it remained constant, in contrast with the partial reversal noted above for bisoxonol at low-medium peptide concentrations. This is because SYTOX® fluorescence involves high affinity binding to nucleic acids, amounting to practical irreversibility, whereas bisoxonol insertion into the membrane hydrophobic matrix is dynamic and reversible. Taken together, these results evidenced that below 2 μM the peptide induced a transient, concentration-dependent membrane depolarization. These transitory lesions might allow some SYTOX molecules to gain access to the intracellular milieu.

### 3.2. Induction of NF-κB and NOS2 by CA(1–8)M(1–18 ) in RAW 264.7 cells

In a previous work, we described the induction of NOS2 expression in RAW 264.7 caused by CA(1–8)M(1–18). In order to link this effect to those concerning plasma membrane permeation, we independently transfected two set of cells with two expression vectors, each encoding luciferase as reporter gene, either under a murine NOS2 promoter, or with one containing three κB sites, whereby its activation became highly dependent on the NF-κB activation. Under these conditions,

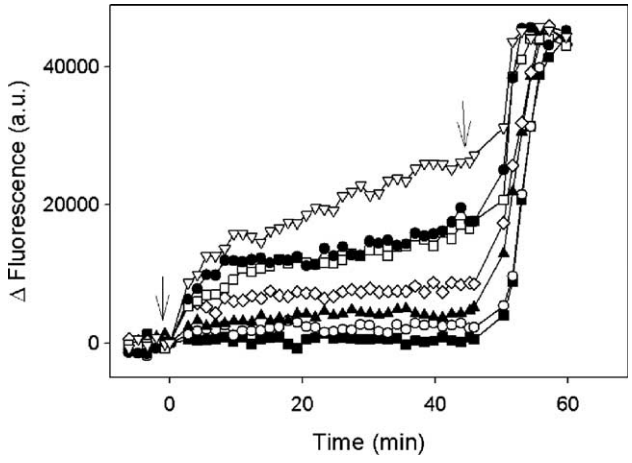


Fig. 2. Permeation of RAW 264.7 cells to the vital dye SYTOX® green caused by addition of CA(1–8)M(1–18). Peptide was added to cells ($10^5$ cells/well) in the presence of 1 μM SYTOX® green in PBS + 20 mM D-glucose and the increase in fluorescence ($\lambda_{exc}$=485 nm, $\lambda_{em}$=520 nm) monitored. Control cells: solid squares. Peptide CA(1–8)M(1–18): 0.1 μM, empty circles; 0.2 μM, solid triangles; 0.5 μM, empty diamonds; 0.7 μM, empty squares, 1.0 μM, solid circles; 2.0 μM, empty triangles. First and second arrows stand for peptide and 0.05% Triton X-100 addition, respectively. Figure is representative of three other experiments performed independently.

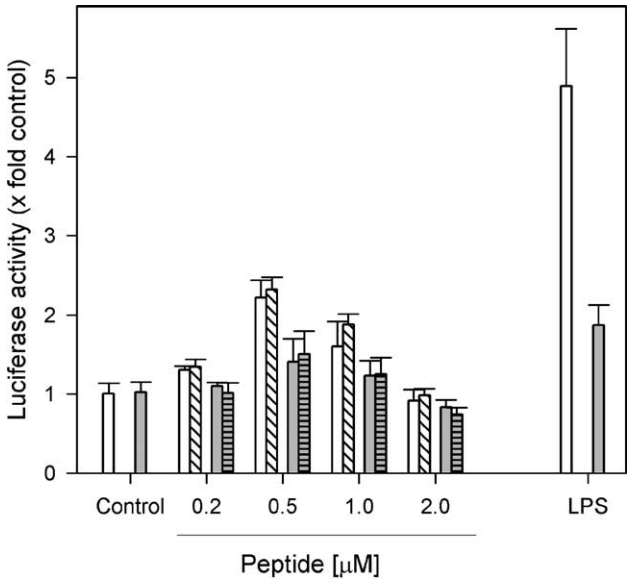


Fig. 3. NF-κB and NOS2 promoter activity in RAW 264.7 cells incubated with CA(1–8)M(1–18). The activity of luciferase as reporter gene was measured in two separate sets of RAW cells ($6\times10^5$ cells/well), lipofected either with the expression vector piNOSLuc, encoding luciferase under the proximal region of the murine promoter for NOS2 (white bars), or with pNF3ConA—where the promoter of luciferase contains three copies of the κB consensus from the immunoglobulin kappa-chain promoter (gray bars). The stimuli for luciferase expression are shown at the abscissa: Control, unstimulated cells; Peptide, CA(1–8)M(1–18) (plain bars) or its all-D-enantiomer (hatched bars); standard inducer, LPS, 1 μg/mL. The results were normalized with respect to luciferase activity of untreated cells (control) with ±S.D.

luciferase expression induced by CA(1–8)M(1–18) or its all-D-enantiomer paralleled that of NOS2. The expression of luciferase, measured at three peptide concentrations, is shown in Fig. 3. At 0.5 μM, the concentration causing the maximal NOS2 expression with minimal toxicity, the expression of luciferase, under NOS2 or κB promoter respectively, was 2.2 (±0.3) and 1.4 (±0.3)-fold higher than the unstimulated control cells. In agreement with previous data [25], the induction of these genes was always lower than that caused by 1 μg/mL of LPS: 4.9 (±0.8) and 1.9 (±0.3)-fold higher relative to unstimulated cells. Interestingly, the all-D-enantiomer of CA(1–8)M(1–18) caused a similar or even a slightly higher activity than an all-L-amino acid synthetic peptide, ruling out the involvement of a chiral receptor (Fig. 3). At this range of peptide concentrations, the maximal inhibition of RAW 264.7 was less than 15% of the control cells.

### 3.3. Binding of fluoresceinated CA(1–8)M(1–18) to RAW 264.7

The fluoresceinated CA(1–8)M(1–18) analogue showed a concentration-dependent accumulation into RAW 264.7 cells. After 4-h incubation, the number of peptide molecules bound per RAW 264.7 cell was $(7.7\pm1.2)\times10^6$, $(15.6\pm2.3)\times10^6$, and $(37.4\pm3.9)\times10^6$ at 0.5, 1.5 and 4 μM, respectively. In a kinetics experiment, the maximal level of fluorescence was always observed during the initial 5 min, regardless of the concentration assayed (data not shown).

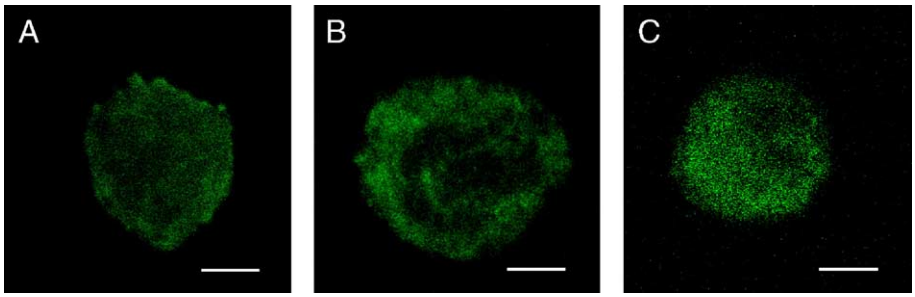


Fig. 4. Confocal microscopy of RAW 264.7 cells labeled with fluoresceinated CA(1–8)M(1–18). Cells were plated as above and incubated with 0.5 (A), 1.5 (B) and 4.0 μM (C) fluoresceinated CA(1–8)M(1–18) for 4 h at 37 °C. Cells were observed in a Leica TCS-SP2-AOBS-UV confocal microscope equipped with inverted optics ($\lambda_{exc}$=482 nm and $\lambda_{em}$=519 nm). Peptide binding stoichiometry was 7.7 (±1.2) × $10^6$, 15.6 (±2.3) × $10^6$, and 37.4 (±3.9) × $10^6$ molecules/cell at 0.5, 1.5 and 4 μM, respectively. Scale bar=4 μm.

By confocal microscopy, the fluoresceinated CA(1–8)M(1–18) appeared as small patches (Fig. 4), and completely different from the more homogenous pattern obtained upon labeling the cells with CFSE, a passive membrane-permeable fluorescein derivative that reacts with amine groups, including intracellular ones [35]. Three-dimensional single cell image reconstruction by composition of serial confocal sections through the z axis showed a staining of the irregular surface of the macrophages by fluoresceinated CA(1–8)M(1–18), rather than the more uniform distribution achieved by CFSE labeling, which includes the intracellular space (see Supplemental material).

### *3.4. Electrophysiological effects of CA(1–8)M(1–18) on RAW 264.7 cells*

In order to get a deeper insight into the plasma membrane permeation described in the previous subsections, we analyzed the ion currents of RAW 264.7 cells in the presence of 0.5 μM CA(1–8)M(1–18). We choose this concentration since it produced maximal depolarization and expression of NOS2 yet minimal cytotoxicity. Under basal conditions, RAW 264.7 cells only exhibited an inward rectifying current and an outward current (Figs. 5A and 5B). After applying pulse protocols used to activate either $Ca^{2+}$ or $Na^{+}$ channels (200 ms

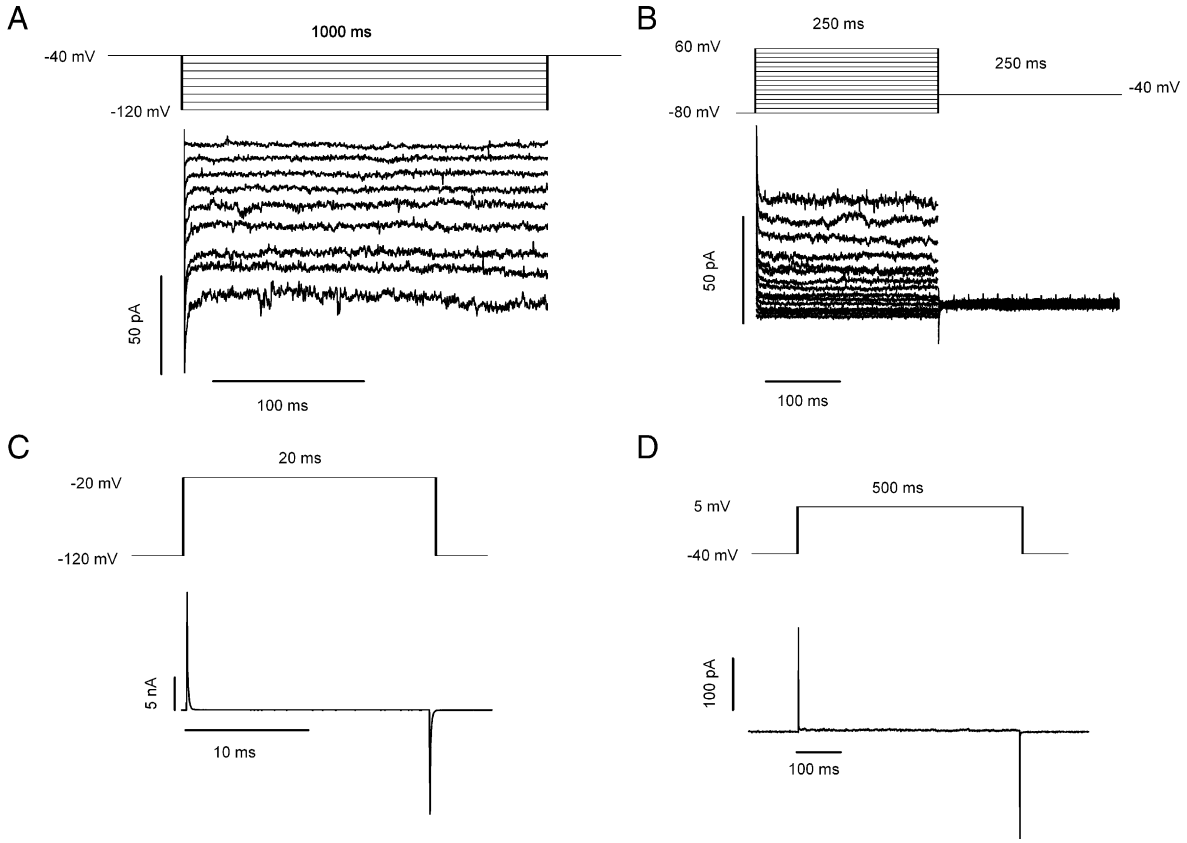


Fig. 5. Endogenous currents recorded in RAW 264.7 cells after applying different pulse protocols. (A) Pulse protocol used to record inward rectifying currents. (B) Pulse protocol used to record outward delayed rectifier currents. (C) Pulse protocol used to record $Na^{+}$ current. (D) Pulse protocol used to record $Ca^{2+}$ current.

from −40 to +50 mV in 10 mV steps, and 25 ms from −120 to +50 mV in 10 mV steps, respectively), no current with such electrophysiological characteristics was recorded (Fig. 5C and D), in agreement with data previously described [36–38].

Therefore, the experiments were carried out after applying ramps from −100 mV to +140 mV (24 mV/s) in order to record the overall cell current. Fig. 6 shows the current generated under such pulse protocols in the absence and in the presence of 0.5 μM CA(1–8)M(1–18). In the absence of the peptide, an inward current was observed, followed by an outward one with a mean amplitude value of 797.5±244.3 pA ($n$=6). In less than 1 min after cell perfusion with 0.5 μM CA(1–8)M(1–18), the cell conductance increased dramatically (Fig. 6). After 10 min, the recorded currents saturated the amplifier. These effects were observed upon continuous perfusion of the cells with CA(1–8)M(1–18). However, as depicted in Fig. 7, once cell perfusion stopped, the amplitude of the current decreased, to increase again upon re-start of peptide flux. This reversibility was in full agreement with the previous results on plasma membrane potential variation.

The effects caused by CA(1–8)M(1–18) may be due either to a very high increase of the endogenous currents, or to unspecific membrane permeation. In order to discern between these two possibilities, we compared the outward and inward currents in the absence and the presence of CA(1–8)M(1–18), by using pulse protocols that activate these currents. Fig. 8 shows the current recorded in the absence and in the presence of 0.5 μM CA(1–8)M(1–18). It can be seen that these two currents were not modified by the peptide, thus suggesting that CA(1–8)M(1–18) effects are not due to an increase of any of these two endogenous currents, but to unspecific membrane permeation. In fact, Triton X-100 (a non- specific permeation agent) at 0.01% induced qualitatively similar effects as 0.5 μM CA(1–8)M(1–18) (Fig. 9). The fact that CA(1–8)M(1–18) effects can be attributed to unspecific membrane permeation rather than to a specific effect on a given ion channel may be

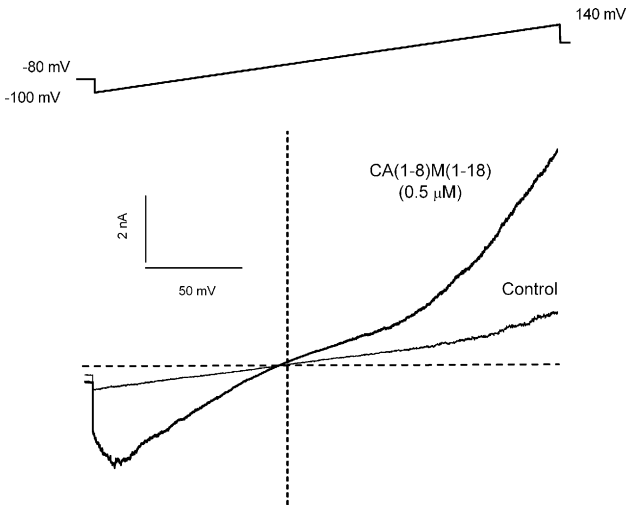


Fig. 6. Effects of CA(1–8)M(1–18) on the current–voltage relationship obtained in control conditions and in the presence of 0.5 μM peptide. Pulse protocol, shown on the top panel, consists in a ramp from −100 mV to +140 mV. Holding potential was maintained at −80 mV.

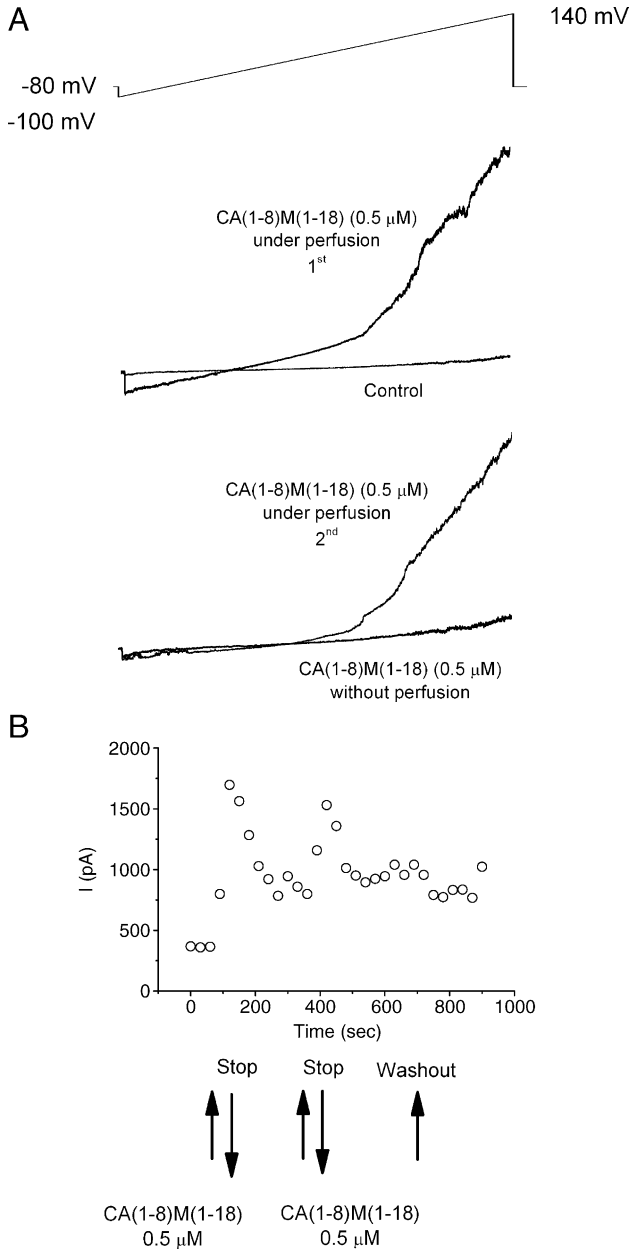


Fig. 7. Variation in the currents recorded in RAW 264.7 cells in the absence and in the presence of CA(1–8)M(1–18) under different perfusion conditions. Panel A: Pulse protocol, shown on the top panel, consisted in a ramp from −100 mV to +140 mV. Holding potential was maintained at −80 mV. Records were obtained in the absence and in the presence of 0.5 μM CA(1–8)M(1–18) under continuous perfusion of external peptide solution. The bottom panel shows a ramp obtained in the presence of CA(1–8)M(1–18) under continuous perfusion and after stopped flow (without perfusion). Panel B: Variations in current amplitude vs. time of a representative experiment. During this period, control conditions (at the beginning), perfusion with CA(1–8)M(1–18), and stop of perfusion are indicated by arrows.

easily fit into two of the currently accepted models of membrane permeation by EAPs, namely the carpet-like and the two-state or worm-hole mechanisms [4].

## 4. Discussion

In the present work, we report the electrophysiological and permeating effects of CA(1–8)M(1–18), a synthetic cecropin

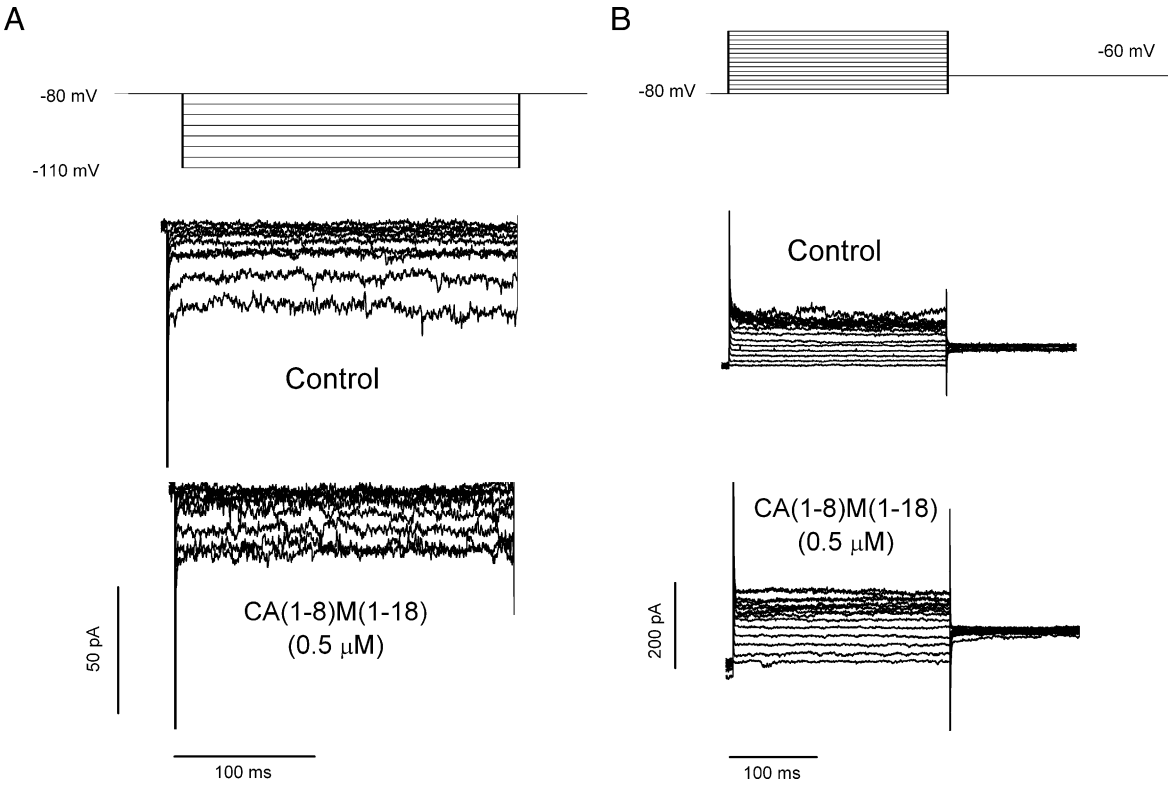


Fig. 8. Effects of CA(1–8)M(1–18) on the endogenous currents of RAW 264.7 cells. Current records obtained in the absence and in the presence of the peptide after applying a pulse protocol that activates an inward current (A) or a delayed outward current (B). Holding potential was maintained at −80 mV in both experiments.

A–melittin hybrid antibiotic peptide [39], on the RAW 264.7 murine macrophage cell line. The peptide produced a significant variation in the levels of expression of some murine macrophage genes [25,40], including the induction of NOS2 in the absence of any other stimuli [25]. The signal transduction pathways involved in this process have been only partially mapped, i.e., there is an increase in the levels of intracellular $Ca^{2+}$ after peptide addition, and activation of the NF-κB pathway is essential to the process [25]. As these effects were reproducible with the all-D enantiomer, this strongly suggested membrane permeabilization as an early step in NOS2 induction, which is studied in detail in the present work. Despite minor quantitative differences between our earlier results [25] and the present ones, our original conclusions remain unaltered.

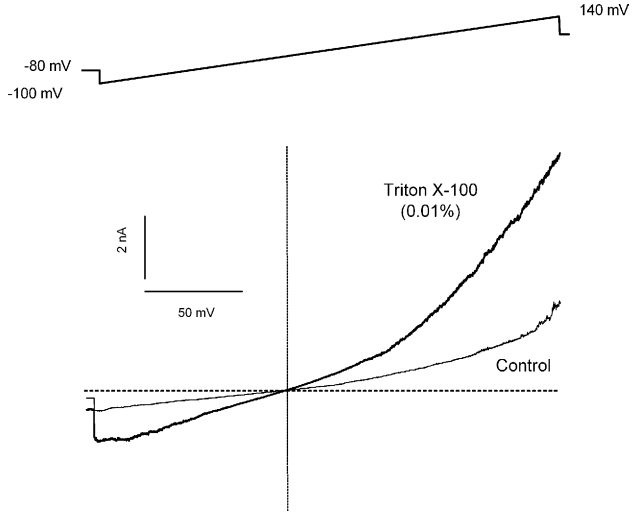


Fig. 9. Effects of Triton X-100 (0.01%) on the current recorded in RAW 264.7 cells. Pulse protocol, shown on the top panel, consisted in a ramp from −100 mV to +140 mV. Holding potential was maintained at −80 mV. Note that the detergent induces an effect qualitatively similar to that of CA(1–8)M(1–18).

Once the reproducibility of the results was ensured, we examined the early steps underlying the process. Our results show that CA(1–8)M(1–18) causes an non–selective but transitory permeation of the RAW 264.7 plasma membrane to ions at 0.5 μM, the optimal concentration for depolarization of RAW 264.7 and NOS2 induction with minimal toxicity [25,41]. This was evidenced by the electrophysiological effects induced by CA(1–8)M(1–18) on RAW 264.7 cells: macrophage permeability ceased when the flux of the peptide solution into the perfusion chamber was stopped. Similar conclusions were drawn in depolarization experiments, although in this case the peptide was added as a single dose rather than in a continuous flow. At low-medium peptide concentrations, a fast initial and partially reversible depolarization was observed, of an extent directly related to peptide concentration. The time and degree of the repolarization of the plasma membrane was inversely related to the dose of peptide, and above 2.0 μM the damage became largely irreversible.

The pattern of the electrophysiological effects of CA(1–8)M(1–18) on RAW 264.7 fitted with an unspecific ionic

permeabilization rather than with the involvement of specific channels. CA(1–8)M(1–18) at 0.5 μM induced an increase in membrane conductance that disappeared when the flow was stopped. One may conclude from this that CA(1–8)M(1–18)-induced membrane perturbation, including $Ca^{2+}$ entrance into the cytoplasm [25] evidenced by the above mentioned increase in cell conductance, is directly responsible for macrophage activation. This is further supported by our finding that NOS2 induction by CA(1–8)M(1–18) and LPS required ionic fluxes through the plasma membrane of the macrophage, though the effects and mechanisms for either compound differed widely. First, the level of NOS2 induction by the peptide was consistently lower than those obtained with LPS or inflammatory cytokines. One must therefore conclude that, under physiological conditions, the antiendotoxic effect of the peptide, which is known to preclude LPS binding to the CD14 receptor [42], will prevail over any small NOS2 induction it may cause, with a final-anti inflammatory outcome [43–45]. Secondly, the ionic fluxes required for NOS2 induction by LPS involve voltage-specific potassium channels, mainly Kv1.3 and Kir2.1, whose expression level varies after LPS binding to the corresponding Toll receptor [37]. In contrast, the mild induction of NOS2 by CA(1–8)M(1–18) was achieved by unspecific perturbation of the macrophage plasma membrane, most likely by stoichiometric interaction of the peptide with the phospholipids of the outer leaflet. This NOS2 induction is reproducible with the all-D (enantiomeric) peptide, [37,46] and endowed with a poor modulation, evidenced by the narrow concentration gap between the NOS2 induction and the trigger of apoptosis. In fact, the outward currents induced by CA(1–8)M(1–18) in RAW 264.7 cells were qualitatively similar to those induced by Triton X-100, a detergent that permeabilizes the cell membrane, thus suggesting an activation of RAW 264.7 cells following an unspecific membrane permeation, possibly similar to that proposed for other membrane-active EAPs, such as human β-defensin 3 on *Xenopus* oocytes [13]. Changes in the ionic condition of the extracellular medium, such as low pH, have also been described as inducers of NOS2 expression in rat macrophages [47].

Our results substantiate the unspecific permeation by an EAP of a higher eukaryotic cell, a fact that somehow challenges the earlier assumption of an exclusive specificity of action of these antibiotic peptides on pathogens. Indeed, a variety of EAPs have been described as capable of affecting different classes of cells sharing a common receptor, with promotion of chemotaxis, angiogenesis and immune differentiation [8]. Interestingly, unspecific permeation by EAPs of diverse amphibian and mammalian cells has been also reported [12–14], sometimes underlying a physiological function such as the IL-1β processing [18], or induction of vascular permeability by neutrophils [17]. The induction of NOS2 expression on RAW 264.7 by CA(1–8)M(1–18) [25], a peptide capable of inducing permeability on zwitterionic liposomes [26], fits into this category. However, there are significant differences between the permeation processes for liposomes and macrophages. First, permeation of RAW 264.7 cells required continuous perfusion with the peptide to maintain its effect, whereas for zwitterionic liposomes a single dose of CA(1–8)M(1–18) caused an increasing and irreversible leakage of the intracellular contents of the liposome. Secondly, while for liposomes there were no significant differences in the release of dyes of broadly different sizes [26], in the macrophage the extent of plasma membrane permeation differed widely between monovalent ions (i.e., depolarization) and the MW 900 SYTOX® green dye.

These differences clearly suggest that CA(1–8)M(1–18) may act through different permeabilization mechanisms. Thus, for zwitterionic liposomes, a carpet-like mechanism was proposed [26] where release of vesicle content was caused by reversible but productive temporary distortions in phospholipid packing. However, as the CA(1–8)M(1–18) interaction with the zwitterionic bilayer was of low affinity, the process was reversible and allowed the peptide to interact with other liposomes. In contrast, in the present patch-clamp and depolarization experiments on macrophages, this effect of recurring permeabilization was absent, as permeabilization stopped with the peptide supply. This might result from peptide degradation by trypsin-like proteinases from the macrophage, but seems somewhat unlikely since supplementing the peptide solution with 5 μg/mL of trypsin inhibitor did not alter the situation (data not shown). Alternatively, it can be explained by a permeabilization mechanism based on the worm-hole or two-state model [48,49]. Under this hypothesis, permeabilization is achieved by formation of mixed peptide–phospholipid transient pores of variable stoichiometry that deactivate spontaneously, distributing peptide monomers at both sides of the membrane. This model will account for the reversibility of the permeabilization and depolarization effects, as well as for the fact that an influx of fresh peptide is required to maintain permeabilization. The adoption of either model is highly dependent on additional factors such as the complexity of biological vs. model membranes, or the existence of a membrane potential in the macrophage, but not in liposomes, that favors formation and stabilization of the membrane-spanning pore [50]. In fact, even with model planar membranes containing acidic phospholipids more prone to be permeated by cationic peptides, a membrane potential was needed to set off permeation by CA(1–8)M(1–18) (named CEME in that particular work [51]).

Assuming that the worm-hole mechanism underlies the effects observed on macrophages, an intrinsic consequence of pore deactivation would be the translocation into the cytoplasm of peptide molecules that could gain access to intracellular targets. Since the all-D CA(1–8)M(1–18) enantiomer reproduces the effect, this hypothesis can be ruled out. In fact, the three-dimensional distribution of fluoresceinated CA(1–8)M(1–18) is quite different from that of CFSE, which also labels the cytoplasm (see Supplemental material). The binding stoichiometry of the fluoresceinated peptide at 0.5 μM, that concentration providing optimal effect/toxicity ratio, was estimated as $7 \times 10^6$ molecules/cell. For melittin, permeability to $Na^+$ in human red blood cells was achieved at $2 \times 10^4$ molecules/cell [52]. Correcting for the differences in area between human erythrocytes and macrophages (120 and 1300 $\mu m^2$, respectively;

[53]), the density of melittin molecules required for permeabilization would be $2 \times 10^5$ molecules/cell. Therefore, a peptide density at least 30-fold higher is required for NOS2 induction by CA(1–8)M(1–18) than for erythrocyte permeabilization by melittin. This estimation fully agrees with the lower cytotoxicity of CA(1–8)M(1–18) relative to melittin [39].

As mentioned in Introduction, modulation of the immune cells by unspecific permeation by EAPs was recently described for LL-37 on IL-1β processing in macrophages [18]. Nevertheless, the in vivo toxic effects of these peptides will be strongly modulated by their short life in serum, either by degradation by proteinases or through their binding to serum proteins [39,54–56], as well as by interaction with anionic components of the membrane, mainly glycosaminoglycans [57]. In fact, a complete lack of toxicity was described for cecropin A–melittin peptides, such as the CA(1–7)M(2–9) hybrid, when applied as a colirium against experimental ocular keratitis in rabbits [23], or of its acylated analogue, $N^{\alpha}$-octanoyl-CA(1–7)M(2–9), administered by intravenous injection in *Leishmania*-infected dogs [24]. Experiments are in progress in order to define whether NOS2 induction was solely due to variation of ionic gradients across the membrane or to the release of intracellular mediators, as described for IL-1 processing driven by LL-37 [18].

In conclusion, our results demonstrate immune cell modulation by EAPs or their analogues causing unspecific but limited permeation of the plasma membrane, in contrast with modulation through EAP–receptor interaction as described for the defensins [7]. The importance of the macrophage in the modulation of the immune response against a wide variety of pathogens, plus the fact that CA(1–8)M(1–18) can activate this cell to express nitric oxide, a lethal metabolite for a wide variety of pathogens, even in the absence of other cytokines, open new therapeutic perspectives for these peptides aside from their permeation of pathogen surfaces.

## Acknowledgments

This work was supported by Spanish Ministries of Health (FIS grants 01/113, PI0408827 and PI0408850 and Redes Temáticas de Investigación Cooperativa C03/01 and C03/14) and Education and Science (grants SAF2002-02160, SAF2004-06856, BIO2002-04091-C03-01, BIO2003-09056-CO2-O2) and by Comunidad Autónoma de Madrid (grant GR/SAL/0854/2004). The authors thank Drs. Antonio Felipe and Rubén Vicente for their helpful discussions, and Guadalupe Pablo for excellent technical assistance.

## Appendix A. Supplementary data

Supplementary data associated with this article can be found in the online version at doi:10.1016/j.bbamcr.2005.11.003.

## References

[1] D. Yang, A. Biragyn, L.W. Kwak, J.J. Oppenheim, Mammalian defensins in immunity: more than just microbicidal, Trends Immunol. 23 (2002) 291–296.
[2] M.R. Yeaman, N.Y. Yount, Mechanisms of antimicrobial peptide action and resistance, Pharmacol. Rev. 55 (2003) 27–55.
[3] A. Tossi, L. Sandri, A. Giangaspero, Amphipathic, alpha-helical antimicrobial peptides, Biopolymers 55 (2000) 4–30.
[4] Y. Shai, Mode of action of membrane active antimicrobial peptides, Biopolymers 66 (2002) 236–248.
[5] D. Andreu, L. Rivas, Animal antimicrobial peptides: an overview, Biopolymers 47 (1998) 415–433.
[6] K. Matsuzaki, Magainins as paradigm for the mode of action of pore forming polypeptides, Biochim. Biophys. Acta 1376 (1998) 391–400.
[7] D. Yang, A. Biragyn, D.M. Hoover, J. Lubkowski, J.J. Oppenheim, Multiple roles of antimicrobial defensins, cathelicidins, and eosinophil-derived neurotoxin in host defense, Annu. Rev. Immunol. 22 (2004) 181–215.
[8] B.B. Finlay, R.E. Hancock, Can innate immunity be enhanced to treat microbial infections? Nat. Rev., Microbiol. 2 (2004) 497–504.
[9] Y. Murakami, H. Nagata, S. Shizukuishi, K. Nakashima, T. Okawa, M. Takigawa, A. Tsunemitsu, Histatin as a synergistic stimulator with epidermal growth factor of rabbit chondrocyte proliferation, Biochem. Biophys. Res. Commun. 198 (1994) 274–280.
[10] F. Niyonsaba, H. Ushio, I. Nagaoka, K. Okumura, H. Ogawa, The human beta-defensins (-1, -2, -3, -4) and cathelicidin LL-37 induce IL-18 secretion through p38 and ERK MAPK activation in primary human keratinocytes, J. Immunol. 175 (2005) 1776–1784.
[11] R. Koczulla, G. von Degenfeld, C. Kupatt, F. Krotz, S. Zahler, T. Gloe, K. Issbrucker, P. Unterberger, M. Zaiou, C. Lebherz, A. Karl, P. Raake, A. Pfosser, P. Boekstegers, U. Welsch, P.S. Hiemstra, C. Vogelmeier, R.L. Gallo, M. Clauss, R. Bals, An angiogenic role for the human peptide antibiotic LL-37/hCAP-18, J. Clin. Invest. 111 (2003) 1665–1672.
[12] B. Haimovich, J.C. Tanaka, Magainin-induced cytotoxicity in eukaryotic cells: kinetics, dose-response and channel characteristics, Biochim. Biophys. Acta 1240 (1995) 149–158.
[13] J.R. Garcia, F. Jaumann, S. Schulz, A. Krause, J. Rodriguez-Jimenez, U. Forssmann, K. Adermann, E. Kluver, C. Vogelmeier, D. Becker, R. Hedrich, W.G. Forssmann, R. Bals, Identification of a novel, multifunctional beta-defensin (human beta-defensin 3) with specific antimicrobial activity. Its interaction with plasma membranes of *Xenopus* oocytes and the induction of macrophage chemoattraction, Cell Tissue Res. 306 (2001) 257–264.
[14] M.E. Mangoni, A. Aumelas, P. Charnet, C. Roumestand, L. Chiche, E. Despaux, G. Grassy, B. Calas, A. Chavanieu, Change in membrane permeability induced by protegrin 1: implication of disulphide bridges for pore formation, FEBS Lett. 383 (1996) 93–98.
[15] W.I. Lencer, G. Cheung, G.R. Strohmeier, M.G. Currie, A.J. Ouellette, M.E. Selsted, J.L. Madara, Induction of epithelial chloride secretion by channel-forming cryptdins 2 and 3, Proc. Natl. Acad. Sci. U. S. A. 94 (1997) 8585–8589.
[16] P.W. Lin, P.O. Simon Jr., A.T. Gewirtz, A.S. Neish, A.J. Ouellette, J.L. Madara, W.I. Lencer, Paneth cell cryptdins act in vitro as apical paracrine regulators of the innate inflammatory response, J. Biol. Chem. 279 (2004) 19902–19907.
[17] N. Gautam, A.M. Olofsson, H. Herwald, L.F. Iversen, E. Lundgren-Akerlund, P. Hedqvist, K.E. Arfors, H. Flodgaard, L. Lindbom, Heparin-binding protein (HBP/CAP37): a missing link in neutrophil-evoked alteration of vascular permeability, Nat. Med. 7 (2001) 1123–1127.
[18] A. Elssner, M. Duncan, M. Gavrilin, M.D. Wewers, A novel P2X7 receptor activator, the human cathelicidin-derived peptide LL37, induces IL-1 beta processing and release, J. Immunol. 172 (2004) 4987–4994.
[19] L. Rivas, D. Andreu, Cecropin-melittin hybrid peptides as versatile templates in the development of membrane-active antibiotics agents, in: G. Menestrina, M. Dalla Serra (Eds.), Pore-Forming Peptides and Protein Toxins, Harwood Academic Publishers, Reading Berkshire UK, 2003, pp. 215–259.
[20] H.G. Boman, D. Wade, I.A. Boman, B. Wahlin, R.B. Merrifield, Antibacterial and antimalarial properties of peptides that are cecropin-melittin hybrids, FEBS Lett. 259 (1989) 103–106.
[21] P. Diaz-Achirica, J. Ubach, A. Guinea, D. Andreu, L. Rivas, The plasma membrane of *Leishmania donovani* promastigotes is the main target for

CA(1–8)M(1–18), a synthetic cecropin A–melittin hybrid peptide, Biochem. J. 330 (1998) 453–460.
[22] M. Gough, R.E. Hancock, N.M. Kelly, Antiendotoxin activity of cationic peptide antimicrobial agents, Infect. Immun. 64 (1996) 4922–4927.
[23] S. Nos-Barbera, M. Portoles, A. Morilla, J. Ubach, D. Andreu, C.A. Paterson, Effect of hybrid peptides of cecropin A and melittin in an experimental model of bacterial keratitis, Cornea 16 (1997) 101–106.
[24] J. Alberola, A. Rodriguez, O. Francino, X. Roura, L. Rivas, D. Andreu, Safety and efficacy of antimicrobial peptides against naturally acquired leishmaniasis, Antimicrob. Agents Chemother. 48 (2004) 641–643.
[25] M. Velasco, M.J. Diaz-Guerra, P. Diaz-Achirica, D. Andreu, L. Rivas, L. Bosca, Macrophage triggering with cecropin A and melittin-derived peptides induces type II nitric oxide synthase expression, J. Immunol. 158 (1997) 4437–4443.
[26] J.M. Mancheño, M. Onaderra, A. Martinez Del Pozo, P. Diaz-Achirica, D. Andreu, L. Rivas, J.G. Gavilanes, Release of lipid vesicle contents by an antibacterial cecropin A–melittin hybrid peptide, Biochemistry 35 (1996) 9892–9899.
[27] R.B. Merrifield, Solid phase peptide synthesis: I. The synthesis of a tetrapeptide, J. Am. Chem. Soc. 85 (1963) 2149–2154.
[28] G.B. Fields, R.L. Noble, Solid phase peptide synthesis utilizing 9-fluorenylmethoxycarbonyl amino acids, Int. J. Pept. Protein Res. 35 (1990) 161–214.
[29] Q.W. Xie, R. Whisnant, C. Nathan, Promoter of the mouse gene encoding calcium-independent nitric oxide synthase confers inducibility by interferon gamma and bacterial lipopolysaccharide, J. Exp. Med. 177 (1993) 1779–1784.
[30] F. Arenzana-Seisdedos, B. Fernandez, I. Dominguez, J.M. Jacque, D. Thomas, M.T. Diaz-Meco, J. Moscat, J.L. Virelizier, Phosphatidylcholine hydrolysis activates NF-kappa B and increases human immunodeficiency virus replication in human monocytes and T lymphocytes, J. Virol. 67 (1993) 6596–6604.
[31] C.J. Swallow, S. Grinstein, O.D. Rotstein, A vacuolar type H(+)-ATPase regulates cytoplasmic pH in murine macrophages, J. Biol. Chem. 265 (1990) 7645–7654.
[32] M. Colmenares, A. Puig-Kroger, O.M. Pello, A.L. Corbi, L. Rivas, Dendritic cell (DC)-specific intercellular adhesion molecule 3 (ICAM-3)-grabbing nonintegrin (DC-SIGN, CD209), a C-type surface lectin in human DCs, is a receptor for *Leishmania amastigotes*, J. Biol. Chem. 277 (2002) 36766–36769.
[33] O.P. Hamill, A. Marty, E. Neher, B. Sakmann, F.J. Sigworth, Improved patch clamp techniques for high-resolution current recording from cells and cell-free membrane patches, Pflügers Arch. 391 (1981) 85–100.
[34] C. Chicharro, C. Granata, R. Lozano, D. Andreu, L. Rivas, N-terminal fatty acid substitution increases the leishmanicidal activity of CA(1–7)M(2–9), a cecropin-melittin hybrid peptide, Antimicrob. Agents Chemother. 45 (2001) 2441–2449.
[35] C.R. Parish, Fluorescent dyes for lymphocyte migration and proliferation studies, Immunol. Cell Biol. 77 (1999) 499–508.
[36] D.L. Ypey, D.E. Clapham, Development of a delayed outward-rectifying K+ conductance in cultured mouse peritoneal macrophages, Proc. Natl. Acad. Sci. U. S. A. 81 (1984) 3083–3087.
[37] R. Vicente, A. Escalada, M. Coma, G. Fuster, E. Sanchez-Tillo, C. Lopez-Iglesias, C. Soler, C. Solsona, A. Celada, A. Felipe, Differential voltage-dependent K+ channel responses during proliferation and activation in macrophages, J. Biol. Chem. 278 (2003) 46307–46320.
[38] R. Pantoja, J.M. Nagarah, D.M. Starace, N.A. Melosh, R. Blunck, F. Bezanilla, J.R. Heath, Silicon chip-based patch-clamp electrodes integrated with PDMS microfluidics, Biosens. Bioelectron. 20 (2004) 509–517.
[39] D. Wade, A. Boman, B. Wahlin, C.M. Drain, D. Andreu, H.G. Boman, R.B. Merrifield, All-D amino acid-containing channel-forming antibiotic peptides, Proc. Natl. Acad. Sci. U. S. A. 87 (1990) 4761–4765.
[40] M.G. Scott, C.M. Rosenberger, M.R. Gold, B.B. Finlay, R.E. Hancock, An alpha-helical cationic antimicrobial peptide selectively modulates macrophage responses to lipopolysaccharide and directly alters macrophage gene expression, J. Immunol. 165 (2000) 3358–3365.
[41] E. Guerrero, New therapeutic alternatives based on eukaryotic antibiotic peptides in *Leishmania* infections, Doctoral Thesis, School of Pharmacy. Universidad Complutense, 2003.
[42] M.G. Scott, A.C. Vreugdenhil, W.A. Buurman, R.E. Hancock, M.R. Gold, Cutting edge: cationic antimicrobial peptides block the binding of lipopolysaccharide (LPS) to LPS binding protein, J. Immunol. 164 (2000) 549–553.
[43] C.D. Ciornei, T. Sigurdardottir, A. Schmidtchen, M. Bodelsson, Antimicrobial and chemoattractant activity, lipopolysaccharide neutralization, cytotoxicity, and inhibition by serum of analogs of human cathelicidin LL-37, Antimicrob. Agents Chemother. 49 (2005) 2845–2850.
[44] M. Motobu, S. Amer, M. Yamada, K. Nakamura, H. Saido-Sakanaka, A. Asaoka, M. Yamakawa, Y. Hirota, Effects of antimicrobial peptides derived from the beetle *Allomyrina dichotoma* defensin on mouse peritoneal macrophages stimulated with lipopolysaccharide, J. Vet. Med. Sci. 66 (2004) 319–322.
[45] T. Sawa, K. Kurahashi, M. Ohara, M.A. Gropper, V. Doshi, J.W. Larrick, J.P. Wiener-Kronish, Evaluation of antimicrobial and lipopolysaccharide-neutralizing effects of a synthetic CAP18 fragment against *Pseudomonas aeruginosa* in a mouse model, Antimicrob. Agents Chemother. 42 (1998) 3269–3275.
[46] C. Eder, Ion channels in microglia (brain macrophages), Am. J. Physiol. 275 (1998) C327–C342.
[47] A. Bellocq, S. Suberville, C. Philippe, F. Bertrand, J. Perez, B. Fouqueray, G. Cherqui, L. Baud, Low environmental pH is responsible for the induction of nitric-oxide synthase in macrophages. Evidence for involvement of nuclear factor-kappaB activation, J. Biol. Chem. 273 (1998) 5086–5092.
[48] K. Matsuzaki, O. Murase, N. Fujii, K. Miyajima, An antimicrobial peptide, magainin 2, induced rapid flip-flop of phospholipids coupled with pore formation and peptide translocation, Biochemistry 35 (1996) 11361–11368.
[49] H.W. Huang, Action of antimicrobial peptides: two-state model, Biochemistry 39 (2000) 8347–8352.
[50] K. Matsuzaki, O. Murase, K. Miyajima, Kinetics of pore formation by an antimicrobial peptide, magainin 2, in phospholipid bilayers, Biochemistry 34 (1995) 12553–12559.
[51] M. Wu, E. Maier, R. Benz, R.E. Hancock, Mechanism of interaction of different classes of cationic antimicrobial peptides with planar bilayers and with the cytoplasmic membrane of *Escherichia coli*, Biochemistry 38 (1999) 7235–7242.
[52] M.T. Tosteson, S.J. Holmes, M. Razin, D.C. Tosteson, Melittin lysis of red cells, J. Membr. Biol. 87 (1985) 35–44.
[53] H. Bos, W. de Souza, Morphometrical method for estimating mean cell volume of phagocytosing cells, Microsc. Microanal. 7 (2001) 39–47.
[54] A.V. Panyutich, P.S. Hiemstra, S. van Wetering, T. Ganz, Human neutrophil defensin and serpins form complexes and inactivate each other, Am. J. Respir. Cell Mol. Biol. 12 (1995) 351–357.
[55] N. Papo, Y. Shai, New lytic peptides based on the D,L-amphipathic helix motif preferentially kill tumor cells compared to normal cells, Biochemistry 42 (2003) 9346–9354.
[56] K.H. Bartlett, P.B. McCray Jr., P.S. Thorne, Reduction in the bactericidal activity of selected cathelicidin peptides by bovine calf serum or exogenous endotoxin, Int. J. Antimicrob. Agents 23 (2004) 606–612.
[57] A. Schmidtchen, I.M. Frick, L. Bjorck, Dermatan sulphate is released by proteinases of common pathogenic bacteria and inactivates antibacterial alpha-defensin, Mol. Microbiol. 39 (2001) 708–713.